



Research paper

“3Co principle” for fidelity assessment for bulb flat models in ship structural analysis.

Shi Song^{a,*}, Sören Ehlers^b, Moritz Braun^b, Franz von Bock und Polach^a, Aditya Rio Prabowo^c

^a Hamburg University of Technology (TUHH), Institute for Ship Structural Design and Analysis (M-10), Am Schwarzenberg Campus 4 C 21073, Hamburg, Germany

^b German Aerospace Center (DLR), Institute of Maritime Energy Systems, Düneberger Str. 108 21502, Geesthacht, Germany

^c Universitas Sebelas Maret, Surakarta, Indonesia

ARTICLE INFO

Keywords:

Fidelity assessment
Bulb flat
Ship structure
Non-linear analysis
Numerical simulation
Numerical model

ABSTRACT

Although bulb flats have been numerically modelled in many ship structural analysis, whether a bulb flat model should be accepted and applied is seldom discussed. Thus, it is worthwhile to investigate the evaluation of numerical models, which can be accomplished by fidelity assessment. However, there has been no systematic fidelity assessment for bulb flat models. This is due to the absence of sufficient information or assessment strategy. To enable this, in this study, a “3Co principle” is introduced as a framework for the fidelity assessment. Moreover, two bulb flat models, namely the shell-only model and the beam & shell model, are fully described with their relevant data. Following this, the fidelities of these two models are gradually examined using the 3Co principle. It is revealed in this study that, the fidelity of bulb flat model can be systematically assessed via the 3Co principle, together with sufficient information. The results of the presented research are believed to provide a sound basis for the use of bulb flat models in future applications regarding non-linear ship structural analysis.

1. Introduction

The bulb flats, also called as Holland profiles [1,2] (with its short name ‘HP’ for the stiffener type [1–8]), is widely applied in ship structures as stiffeners. In many researches concerning ship collision, grounding, or other non-linear ship structural behaviors, the bulb flats are numerically modelled [4,7–11]. The modelling of a numerical model includes multiple procedures, see Fig. 1. Referring to the modelling procedure shown in Fig. 1, many existing literatures have provided meaningful investigations in different aspects. For example, the bulb flat models by Wilmer III [12] considered the decision of layout and parameters when creating the models. Such consideration was also mentioned by Avi [3] and Bobeldijk [13]. Meanwhile, verification of bulb flat models were carried out via applications in stiffened panels [7, 12,14] or large complex structures [3,4,6,9–11,13]. However, after creation and verification, the decision for acceptance and application should also be discussed. Referring to the benchmark studies for ship structural assessments [15,16], different numerical models, although all properly modelled, have different performances in the same scenario. Hence, it is worthwhile to investigate the evaluation of numerical models. Such evaluation can be accomplished by fidelity assessment for

the numerical models, which reveals their capability of representing corresponding components.

The definition of the term ‘fidelity’ can be seen in many literatures [17–19]. From the view of digital twin, the fidelity of the virtual model should provide the closeness to the physical product [20,21], which is the same for non-linear ship structural analysis. Therefore, a numerical model with suitable fidelity is often favored for the synchronization between the physical and the digital world, [22] and can benefit many numerical applications like numerical simulation, [23–25] optimization [26–28] and machine learning [29–32].

To assess the fidelity of a model, its design and performance should be examined referring to the physical product (called as “real components” in this study). In existing literatures with bulb flat models, the closeness between the models and real components was partly considered or examined. However, none of them provided systematic assessment for the fidelity of the bulb flat models, which is due to the absence of sufficient information or assessment strategy. Without sufficient information, the bulb flat models cannot be rebuilt precisely for assessments. While the information is sufficiently provided, an assessment strategy is required for interpreting the information into fidelity evaluations.

* Corresponding author.

E-mail addresses: shi.song@tuhh.de (S. Song), soeren.ehlers@dlr.de (S. Ehlers), moritz.braun@dlr.de (M. Braun), franz.vonbock@tuhh.de (F. von Bock und Polach), aditya@ft.uns.ac.id (A.R. Prabowo).

<https://doi.org/10.1016/j.rineng.2024.103779>

Received 6 November 2024; Received in revised form 17 December 2024; Accepted 17 December 2024

Available online 19 December 2024

2590-1230/© 2024 The Authors. Published by Elsevier B.V. This is an open access article under the CC BY license (<http://creativecommons.org/licenses/by/4.0/>).

This study aims to provide a way to enable the systematic fidelity assessment for bulb flat models in non-linear ship structural analysis. In Section 2, a framework for fidelity assessment strategy is introduced, which is named as “3Co principle”. The 3Co principle includes three characteristics: correspondence, comparability, and competence. In addition to the 3Co principle, to assess the fidelity of bulb flat models, details of the bulb flat model should be sufficiently described. To achieve this, in this study, two bulb flat models are fully described with their parameters, layouts, configurations in FEM programs, and relevant verifications. In the following sections, the fidelities of these two bulb flat models are gradually assessed in a comparative way, which is suitable for the determination of fidelity [33].

In Section 3, the structure of bulb flats is analyzed. Based on the analysis, the correspondence and the comparability from the 3Co principle are investigated. Then the layout and parameters of bulb flat model are determined considering these two characteristics. After that, the configurations of the bulb flat models in FEM programs are initially discussed. The configurations in FEM programs are further discussed in the following sections, based on their own scenarios.

In Section 4, the presented models are applied in numerical simulations of the bending of bulb flats. The numerical results are verified against analytical results, which shows their competence from the 3Co principle.

From Section 5 to Section 6, the competences of the models are further verified in applications of two more complicated scenarios, which are closely relevant to non-linear ship structural analysis. In Section 5, the scenario is a collision test of a stiffened panel. The numerical results are verified against experimental results and show the competence of the models. In Section 6, the scenario is a collision test of a double hull structure, which can be regarded as a large complex structure. The numerical results are compared with experiment results and existing numerical results to show the competence of the models.

Based on the sections above, in Section 7, the fidelity of bulb flat models for ship structural analysis is discussed from the view of the 3Co principle. Following that, the conclusions from this study are summarized in Section 8.

2. The 3Co principle

To assess the fidelity of a numerical model, according to Carol et al. [34], indicators should be identified, then based on collected information, the indicators are examined in terms of their reliability and validity. In this study, the fidelity of a bulb flat model is composed of three characteristics: correspondence, comparability, and competence, which include multiple indicators respectively. Based on these three characteristics, a framework for the fidelity assessment is presented in this study. This framework is introduced as the “3Co principle”. The characteristics are defined below, while a brief comparison of the three characteristics is shown in Fig. 2.

1. Correspondence: The correspondence represents the closeness between the model and the real components regarding physical parameters. This includes the accuracy of material properties (e.g., density, Young’s modulus, yield strain, etc.), structural properties (e.g., total volume, bending moments, etc.), and so on. The indicators here are suitable for direct quantitative examinations. During the creation of the model, these indicators are checked to guide the creation of the model.
2. Comparability: The comparability represents the closeness when describing the real components with models, such as the outline layout, outline shape, boundary configurations, and so on. Comparing with the correspondence, more qualitative descriptions are required for the indicators from the comparability. Same as above, during the creation of the model, these indicators are checked to guide the creation of the model.
3. Competence: The competence represents the closeness of the performance in application by the model and the real components. This is verified with existing results from the real component in tests, experiments, incidents and so on. The indicators here are relevant on the application scenarios. For example, in non-linear ship structural analysis, the indicators include deflection, force, deformation, energy or movements. Unlike that from the correspondence or comparability, the indicators from the competence cannot be

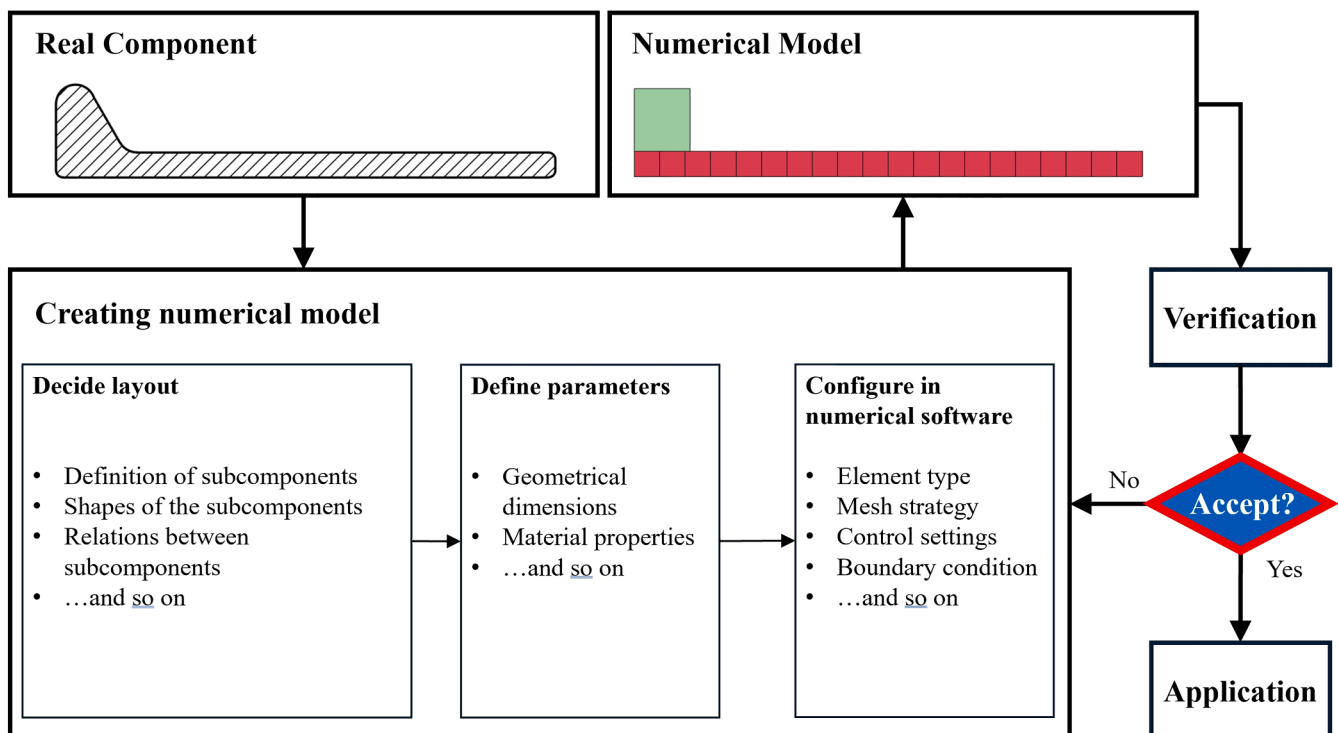


Fig. 1. An example of the modelling procedure of numerical models.

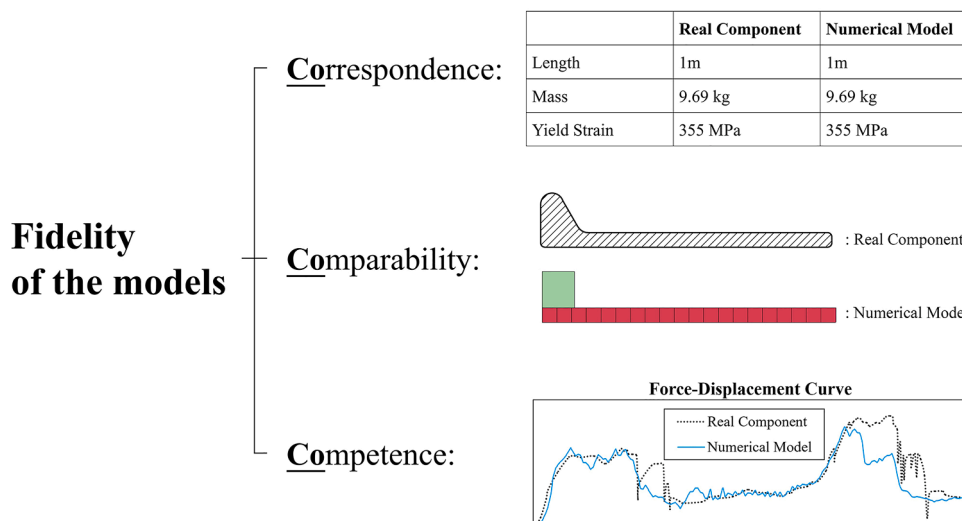


Fig. 2. The three characteristics of fidelity, from the 3Co principle.

instantly checked when creating the models. Nevertheless, if the same model is already examined in similar existing applications, its results can be referred to show the competence of the model.

3. The models of bulb flats

As is mentioned above, without sufficient information, the fidelity of a model cannot be assessed. In this study, the bulb flat models share common features with the models in existing literatures, but are described with full descriptions, including the consideration in layout, definition of parameters, configurations in FEM programs, and so on. This will provide sufficient information for the systematic fidelity assessment. In this section, the structure of bulb flats is analyzed and divided into subcomponents. Then creation of the models is described including outline design, parameter definition and so on. After that, the configuration in numerical software is introduced to finalize the creation of bulb flat models.

3.1. The structure of bulb flats

For a bulb flat, its length is usually much bigger than its height and overall width. Moreover, the cross section of a single bulb flat is supposed to be uniform along the longitudinal direction. Therefore, in this study, the investigation of the bulb flat models is focusing on the modelling of their cross sections, while a whole bulb flat is regarded as a beam structure with the same cross section.

Based on standard ISO 657-19:1980 [35], the cross section of the bulb flat is shown in Fig. 3. Taking the HP-140 × 7 bulb flat as an

example, the values of the parameters for the cross section are shown in Table 1, which is according to ISO 657-19:1980 as well.

In this study, if the numerical model doesn't include the round corners, the total area of the cross-section only increases by 0.069 %. Hence, the round corners are neglected in the bulb flat models. Without the round corners, the cross section of a bulb flat can be regarded as a combination of two subcomponents: a base plate and a 'bulb flange'. In this study, the definitions of the 'bulb flange' and the base plate are shown in Fig. 4.

3.2. The creation of the models

When bulb flats are numerically modelled, three element types can be applied: solid elements, shell elements, or beam elements. In existing literatures concerning non-linear ship structural analysis, shell elements and beam elements are often used, where the bulb flats are either modelled with shell elements only [4,6-8,14], or with the combination

Table 1

The values of the parameters for the cross section of 140 × 7 bulb flat.

Parameter names	Values
b	140 mm
c	19 mm
r	5.5 mm
t	7 mm
r_1	≤ 2 mm

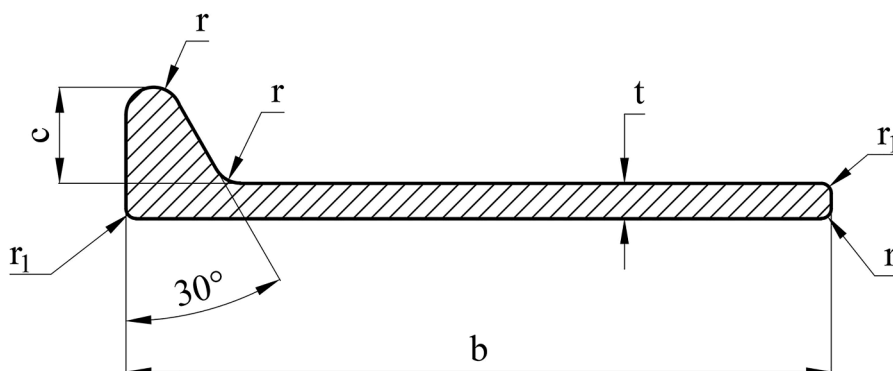


Fig. 3. The cross section and parameters of the bulb flat.

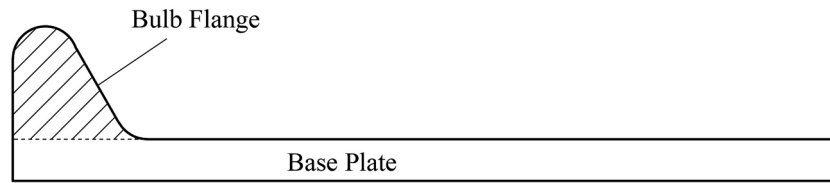


Fig. 4. The two subcomponents of a bulb flat section: bulb flange (the shadow area) and the base plate (white area).

of beam elements and shell elements [13,36]. Comparably, solid elements are often applied when local material behavior, e.g. fatigue, is primarily concerned [1,2,5,37,38]. When beam elements or shell elements are applied, it is difficult to represent curved outlines, thus the geometrical details, such as the rounded corners and circular outlines, cannot be fully described, see Fig. 5. To model the bulb flats with beam elements or shell elements, an ‘idealization’ process is usually needed before the modelling. In the idealization process, the cross-section of the bulb flats are converted into equivalent angle profiles (see Fig. 6), which has been mentioned in existing researches [3,12,39] or technical standards [40,41].

In this study, for the equivalent angle profile, referring to the structure of bulb flats mentioned above, the base plate remains unchanged, while the bulb flange is modelled by an equivalent rectangular flange. From the view of the 3Co principle, although the comparability is therefore reduced, its influence on the fidelity can be minimized. To achieve this, the outline of the equivalent rectangular flange should be investigated.

The outline of the equivalent rectangular flange includes its position and dimension. Regarding the position, the equivalent rectangular flange should be connected to the base plate, while its upper boundary should be aligned with the base plate to avoid worse fidelity (see Fig. 6). In addition to universally recognized parameters (e.g. mass, volume, etc.), more descriptions are required for the position of the equivalent

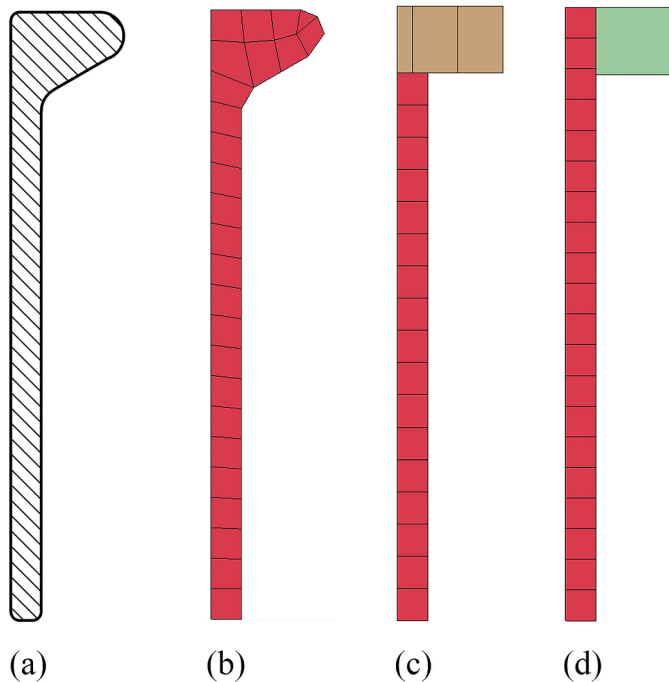


Fig. 5. Comparison of models for a HP-140 × 7 bulb flat using different element types: (a) shows the real geometry of the section of a bulb flat, (b) shows the section of the model by solid elements, (c) shows the equivalent section of the model by shell elements (when the shell thickness is visible), (d) shows the equivalent section of the model by beam and shell elements (when the shell thickness and beam prism are both visible).

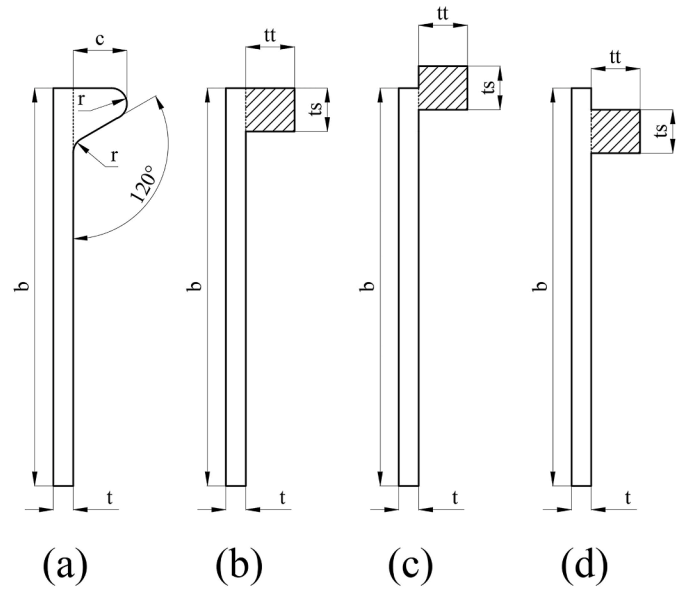


Fig. 6. Outlines of real geometry of a bulb flat (a) and its equivalent angle profile (b), the shadow area in equivalent angle profile is the equivalent rectangular flange. The outlines in (c) and (d) show two examples with worse fidelity regarding the comparability from the 3Co principle.

rectangular flange. Thus, the position here is the indicator included in the comparability from the 3Co principle.

For the cross-section of the equivalent angle profile, the physical attributes include the area and the area moment of inertia, which are used as the indicator included in the correspondence from the 3Co principle. To preserve fidelity, the resultant cross-section should keep its area and area moment of inertia identical or close to that from real components. The dimension of the equivalent rectangular flange consists of the thickness in two directions - the tt and ts (see Fig. 6). To keep the area identical between the model and real components, the relation between tt and ts is described as:

$$tt \times ts = A_{eqf} = A_f \tag{1}$$

where A_{eqf} is the area of equivalent rectangular flange, A_f is the area of the bulb flange.

Based on the parameters mentioned in Table 1, A_f is defined as:

$$A_f = \frac{1}{2}(c - r)^2 \tan \frac{\pi}{6} + \left(\frac{1}{\cos \frac{\pi}{6}} + 1 \right) (c - r)r + \left(\frac{1}{4}\pi + \sin \frac{\pi}{3} \right) r^2 \tag{2}$$

In this section, the HP-140 × 7 bulb flat is selected as an example for investigation. The parameters for the HP-140 × 7 bulb flat are shown in Table 1. From the formula above, for the HP-140 × 7 bulb flat, $A_f = 262.55 \text{ mm}^2$. However, there are still infinite combinations for tt and ts . To determine the parameter among the combinations, investigations are required. Fig. 7 shows the coordinate system defined for a bulb flat in this study. Considering the correspondence from the 3Co principle, the model is compared with the real component with four

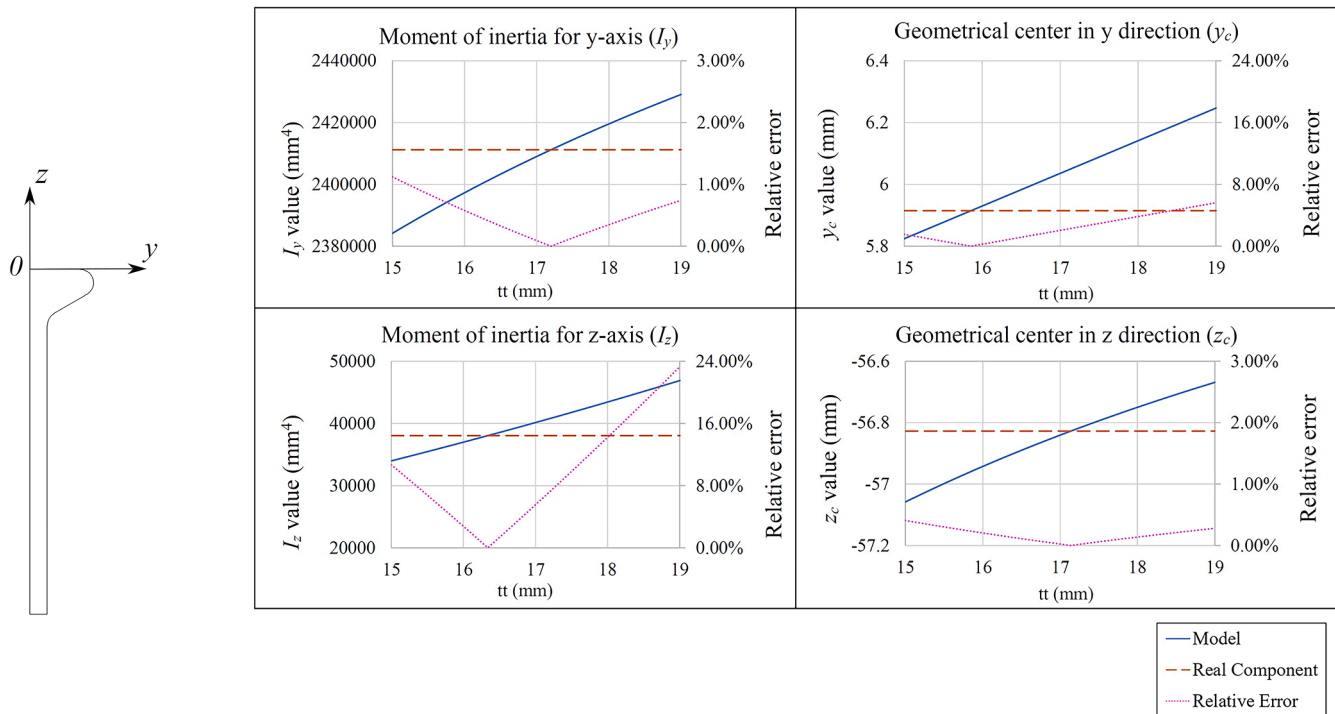


Fig. 7. Coordinate system defined for a bulb flat in this study, as well as the comparison of the properties from the model and the real component.

physical attributes, see Table 2.

The result of the comparison is shown in Fig. 7. The results are calculated by a specifically created scripts using MATLAB R2023a. In the scripts, the tt is searched with a step of 0.000001 mm, with the limitation of $0 < tt \leq 2c$. As is mentioned above, the area of the section is already determined, hence the ts is determined with Eq. 1.

For bulb flats, the load is often applied in a direction close to z-direction, especially in non-linear ship structural analysis, whose load is often from accidental loads like ship collision or grounding [10,42]. Hence, in this study, the z_c and I_y are considered to be more important among the physical attributes, which makes them as the indicators for the correspondence from the 3Co principle. As a result, for the HP-140 \times 7 bulb flat, the values selected are 17.20 mm for tt , and 15.27 mm for ts . By these values, the relative error for z_c and I_y are extremely low, while the relative errors for other parameters are also acceptable, see Table 3.

3.3. The configurations in numerical software

As is mentioned above, when modelling bulb flats, three element types can be applied: solid elements, shell elements, or beam elements. In this section, apart from the model representing real geometry with solid elements, two bulb flat models are represented, which apply shell elements or the combination of beam elements and shell elements, see Table 4.

In this study, the FEM program used for numerical simulation is LS-DYNA version smp-d-R13.1. Meanwhile, the input keyword files are

Table 2 Physical attributes for comparison between the model and the real component.

Property name	Denotation
Mass center in y direction.	y_c
Mass center in z direction.	z_c
Second moment of inertia for y-axis.	I_y
Second moment of inertia for z-axis.	I_z

Table 3 Equivalent geometry dimensions of the bulb flats for verification.

Bulb flat type	tt (mm)	ts (mm)	Relative error against real components:			
			y_c	z_c	I_y	I_z
HP-120 \times 6	15.39	13.79	2.56 %	0.01 %	0.00 %	7.25 %
HP-140 \times 7	17.20	15.27	2.40 %	0.01 %	0.00 %	7.23 %
HP-240 \times 10	30.78	27.57	3.12 %	0.02 %	0.00 %	7.51 %
HP-320 \times 12	41.63	38.07	3.46 %	0.02 %	0.00 %	7.33 %
HP-400 \times 14	52.47	48.57	3.68 %	0.02 %	0.00 %	7.18 %

Table 4 Different bulb flat models in this section.

Model name	Applied elements	Geometry representation
Solid (Real)	Solid elements	Real geometry
Shell-Only	Shell elements	Equivalent geometry
Beam & Shell	Beam elements and Shell elements	Equivalent geometry

created firstly by the LS-PrePost, then enriched by MATLAB scripts. Hence the configurations for numerical software are also based on LS-DYNA and LS-PrePost.

In LS-PrePost, the shell elements can be displayed with their thickness, and the beam elements can be displayed by setting the 'Beam Prism' on. Using these functions, the outline of the models can be displayed, see Fig. 11.

The dimension of the equivalent rectangular flange is same as the selected values above. For correct position of the equivalent rectangular flange, relevant meshing and parameters should be defined. For the mesh of shell-only model, the overall height is $b - ts$, where b is the overall height of the bulb flat. Meanwhile, in *SECTION SHELL from the LS-DYNA keyword, the 'NLOC' is set as ± 1 . Whether its value should be plus or minus is determined by the configuration of the model -e.g., the local coordinate system for shell elements, or the global coordinate

system.

For the explicit calculation in LS-DYNA, the computational cost is relevant to the time step size, which is significantly influenced by minimum element size in the model. Hence, comparing the two ways creating shell-only model, although the higher fidelity model has better correspondence and comparability regarding the 3Co principle (see Fig. 8), the small elements will increase the computational cost. As a result, the shell-only model is created with the lower fidelity model. Therefore, since the beam & shell model does not have such problem, considering the comparability showed in Fig. 6, its fidelity is higher than that from the shell-only model, see Fig. 9. The reduced fidelity from the shell-only model will lead to larger error in sectional parameters along y-axis, such as the position of geometrical center and moment of inertia, by referring to the coordinate system shown in Fig. 7.

For the mesh of beam & shell model, the beam elements are on the top of the mesh of the base plate, while a ‘third node’ is required to define the local coordinate system, see Fig. 10. To assign the correct third node for every beam element, a MATLAB-based scripts is created for this. In *SECTION_BEAM from its LS-DYNA keyword, the ‘NSLOC’ is set as ±1, while the ‘NTLOC’ is defined as:

$$NTLOC = \pm \left(1 + \frac{tt}{t}\right) \quad (3)$$

where t is the thickness of the base plate. For the ‘NSLOC’ and ‘NTLOC’ mentioned above, same as the ‘NLOC’, whether their values should be plus or minus is determined by the configuration of the model -e.g., the local coordinate system for beam elements, or the global coordinate system for the whole model. When correctly defined, the beam & shell model can represent the outline of the equivalent angle profile with high fidelity, which also represent its fidelity of the bulb flat models.

The Solid (Real) model is created using solid elements, based on real geometry. Based on the descriptions above, the numerical models of the HP-140 × 7 bulb flat are shown in Fig. 11.

In this section, during the creation of the model, the determination of the layout or parameters are based on the consideration of the correspondence or the comparability from the 3Co principle. This preserves the fidelity of the models regarding these two characteristics.

Apart from the configurations mentioned above, other parameters or settings in the numerical software also have significant influence on the fidelity. This includes the material model, boundary conditions, dynamic configurations and so on, which are discussed with specific scenarios in the following sections.

4. Fidelity of the models against analytical results

To assess the fidelity of the models, as is mentioned in the first section, the “3Co principle” can be applied. The 3Co principle include three characteristics for the fidelity: correspondence, comparability and

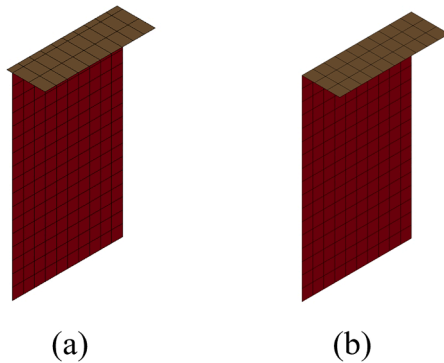


Fig. 8. Higher fidelity shell-only model (a) and lower fidelity shell-only model (b). Compared with the lower fidelity model, the higher fidelity model has elements smaller than normal mesh size.

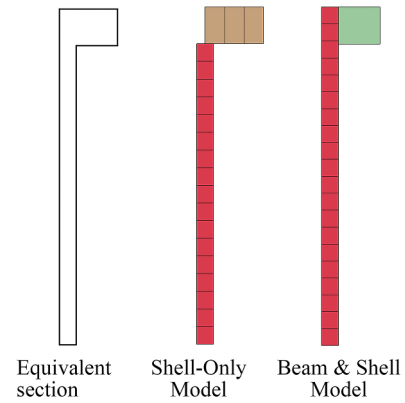


Fig. 9. Comparison of the sections from equivalent angle profile, shell-only model (with lower fidelity) and beam & shell model.

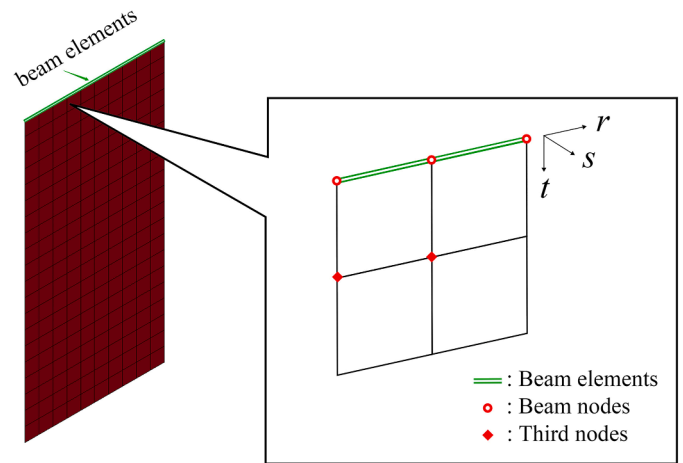


Fig. 10. Configuration of the beam elements, including the assignment of the third nodes.

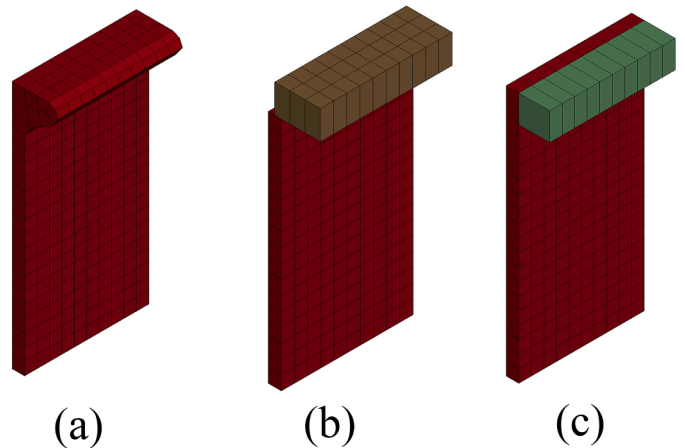


Fig. 11. The HP-140 × 7 bulb flat by the: (a) Solid (Real) model, (b) shell-only model (the shell thickness is displayed), (c) beam & shell model (the ‘Beam Prism’ and shell thickness are displayed). Since the section is the same along the longitudinal direction, only part of the whole bulb flat model (approx. 70mm in longitudinal direction) is shown in this picture.

competence. The correspondence and the comparability are checked during the creation of the models, which are mostly discussed in the last section. Meanwhile, the competence is verified in applications. In this

section, the competences of the presented models are verified against analytical results in application. In the verification, the models are applied to five different types of bulb flats. These bulb flats are listed in Table 5. Details of the bulb flats can be found in standard ISO 657-19:1980 [35].

The verification scenario is the bending of a single-span beam under distributed loading, with its both ends fixed, see Fig. 12. The parameters for the scenarios are shown in Table 5. The lengths of the bulb flats are modelled to be 25–40 times of their height or thickness. Based on the definition in [43], the bulb flats can be regarded as beams in analysis.

In this scenario, the deflections in the middle of the beams (in length direction) are selected as the indicators for the competence from the 3Co principle. Fig. 13 shows the measurement of deflection on the deformed beam. From the Euler–Bernoulli beam theory [44], the analytical result for the selected deflection in z-direction is:

$$v_c = \frac{wL^4}{384EI} \tag{4}$$

where v_c is the z-direction deflection in the middle of the beam ($x = L/2$), w is the distributed load along the beam, L is the length of the beam, I is the second moment of inertia, and E is the Young’s modulus.

In Section 2, the creation of HP-140 × 7 bulb flat model is discussed. Applying the same way creating the models, the dimensions for all bulb flat models are shown in Table 3. In this section, the two models mentioned above – shell-only model and beam & shell model are applied. Moreover, the Solid (Real) model is also applied here as a reference.

For the simulation in LS-DYNA, based on the coordinate system defined in Fig. 7, the displacement of all the nodes in y-direction are constrained to zero. This is intended to avoid the buckling during the loading, and focus on the performance of bending based on Eq. 3. Moreover, to reduce the oscillations and retrieve results at stress equilibrium state, *DAMPING_GLOBAL is applied when the load force reaches desired value – an example is shown in Fig. 14. The material model applied is *MAT_ELASTIC, since no plastic behavior is required here. The physical attributes of the models, such as the material properties (Young’s modulus), structural properties (length of the model) are the same for the analytical and numerical calculations. The boundary conditions are the same for the calculations as well. From the view of the 3Co principle, they show good fidelity of the models regarding the correspondence and comparability respectively.

The comparison between numerical results from different models and analytical results is shown in Table 6. From the comparison, the numerical results are quite close to analytical results. This means, for the presented models, their competence from the 3Co principle is satisfying when representing the bending behavior of the bulb flats.

When creating model for non-linear ship structural analysis, apart from fidelity, applicability is also of great significance. Regarding the computational cost required from these numerical models, the running time for their simulations are considered. For these bulb flat types, under the same conditions from computer (same number of CPU cores are used, no other programs running, etc.), the durations for simulations of shell-only model and beam & shell model are similar. Comparably, the durations for solid elements are about 2 - 6 times of that for shell-only model, or beam & shell model. This means, for the bulb flat models, using only shell elements or the combination of beam and shell elements

Table 5
The bulb flats and the parameters of the scenarios.

Bulb flat type	Length (mm)	Load (kN)	Mesh size (mm)
HP- 120 × 6	3600	10	6
HP- 140 × 7	4000	20	7
HP- 240 × 10	8000	30	10
HP- 320 × 12	12,000	40	12
HP- 400 × 14	16,000	40	14

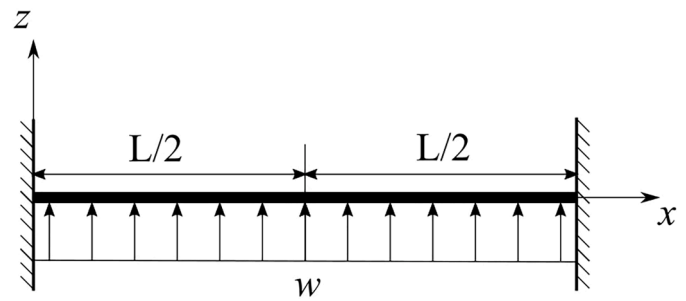


Fig. 12. The loading scenario for verification.

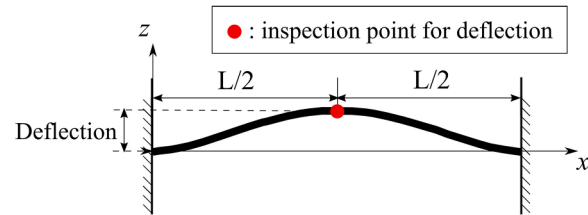


Fig. 13. The measurement of deflection on the deformed beam.

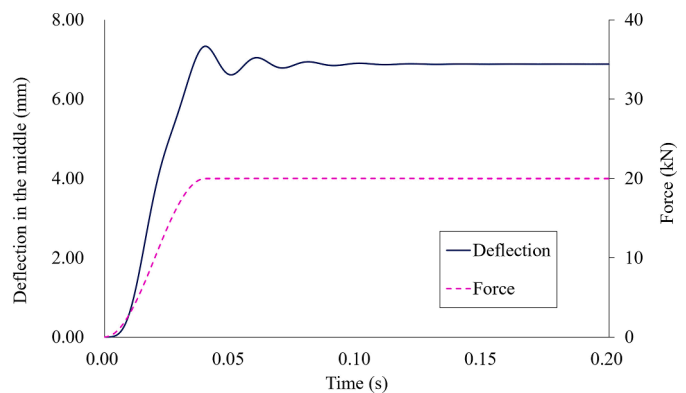


Fig. 14. An example to show the deflection oscillates when the force stops changing, due to the dynamic effect during the loading. When damping is applied, the deflection value will finally converge to stress equilibrium state.

Table 6
Relative error between different models and analytical results.

Models	Solid (Real)	Beam & Shell	Shell-Only
HP- 120 × 6	2.19 %	2.24 %	2.26 %
HP- 140 × 7	2.53 %	2.29 %	2.41 %
HP- 240 × 10	1.96 %	1.82 %	1.72 %
HP- 320 × 12	1.59 %	1.45 %	1.42 %
HP- 400 × 14	1.74 %	1.34 %	1.24 %

requires much less computational cost compared with that using solid elements. As is discussed in existing literatures, such challenges in applying relatively higher fidelity models is possible, and the fidelity of models can be dependent on the use case. [21,45] From the view of the 3Co principle, although the shell-only model and the beam & shell model have relatively lower comparability compared with Solid (Real) model, the idealization process will preserve their fidelity concerning the correspondence. Moreover, these models have good performance and show satisfying competence regarding the 3Co principle. As a result, applying the beam elements or shell elements for bulb flat models is more preferable when considering computational cost. In the following sections, the shell-only model and the beam & shell model are applied.

5. Fidelity of the models in a test of stiffened panel

As is mentioned at the beginning of the last section, based on the 3Co principle, the competence is verified in applications. To verify the competence of the presented models in more complex scenarios, a collision test on a structure stiffened by two bulb flats, represented by Alsos et al. [7,42], is used. In the test, two HP-120 × 6 bulb flats are applied on a stiffened panel. More details concerning the test can be found in the original papers [7,42]. In this study, the numerical model is created mostly with the configurations presented in the original papers [7]. Since the configurations are mostly from the measurement in the experiment, together with that represented in Section 2, the models show good fidelity regarding the correspondence and comparability respectively.

In this study, 2 numerical models are made, with their bulb flats respectively using the shell-only model and the beam & shell model. Fig. 15 and Fig. 16 show the numerical models for the collision test. The parameter for the equivalent angle profile here is the same as that in Table 3.

In these numerical models, the mesh size for the stiffened panel is mostly 5 mm. The exceptions are the ‘welding’ model, which corresponds with that mentioned in the original paper [7]. The stress-strain relationship for the materials is the same as that mentioned in the original paper [7] as well. The boundary conditions are applied by contacting with the boundary structure.

For verification of the competence from the 3Co principle, the post-collision geometry from numerical simulations is chosen as one of the indicators. This includes the deformation shapes, crack shapes, and so on. They are compared with that from the picture in the original paper [42], see Fig. 17. The force-displacement curves from numerical simulations are used as the other indicator. These curves are compared with the experiment result, see Fig. 18. The force-displacement curves from the experiment is retrieved from the original paper [7]. In Fig. 18 that, the beam & shell model shows better performance than the shell-only model regarding the maximum force.

For the comparison of post-collision geometry (see Fig. 17), the most significance difference between the two models is the buckling shape of the bulb flat. Compared with the shell-only model, the buckling shape from beam & shell model corresponds better with the experiment. This can be the main reason for the difference in force-displacement curve from the two models, see Fig. 18.

As is mentioned above, considering computational cost, the shell-only model is created with lower fidelity than the beam & shell model, see Fig. 9. This difference in fidelity is one of the reasons of the different performance from the two models.

6. Fidelity of the models in a test of large complex structure

In this section, for the presented models, their competences from the 3Co principle are verified in a simulation of collision test of large

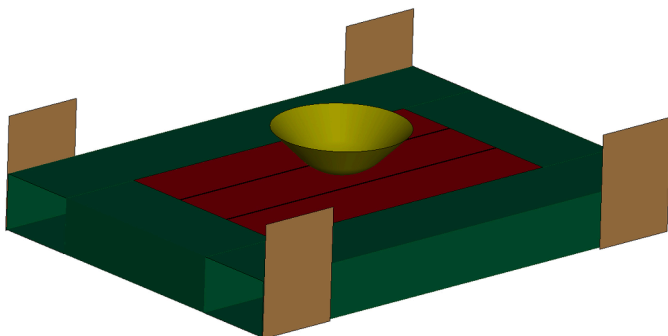


Fig. 15. Numerical model for the scenario. Meshing is not displayed in this picture.

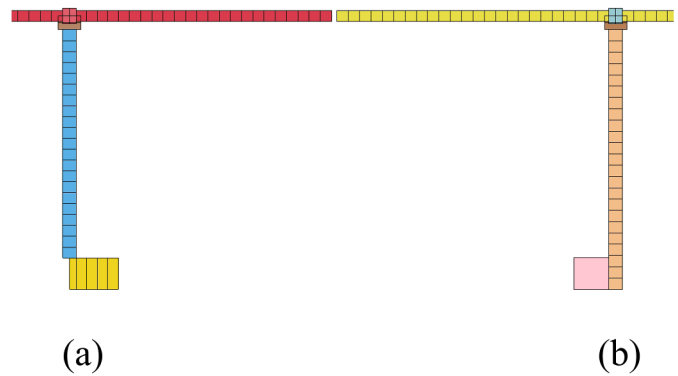


Fig. 16. Cross-section of the bulb flats: (a) by shell-only model. (b) by beam & shell model. The shell thickness and beam prism are displayed here.

complex structure. The scenario for the simulation is based on the large-scale experiment introduced by Fricke et al. [10]. The test set-up is shown in Fig. 19.

In order to control the uncertainties in the comparison with different numerical methods, the configurations for the numerical model are mostly based on that introduced by the relevant work by Kubiczek [11]. The main difference is the bulb flat models and relevant meshing. In this test, the HP-140 × 7 bulb flats are used in the large-scale structure. Since the HP-140 × 7 bulb flat is already investigated above, same configurations for the equivalent angle profile are applied here. In this section, the shell-only model and the beam & shell model are used. The numerical model is shown in Fig. 19, while the equivalent angle profiles for the bulb flats are shown in Fig. 20. The average mesh size for the large structure is 34.2 mm. Since the configurations are mostly from the measurement in the experiment [10,11], such as the dimension of the structure, number and arrangement of subcomponents, boundary conditions, material properties (yield strain, stress-strain curves, etc.), and so on. Hence, together with the that represented in Section 2, from the view of the 3Co principle, the models show good fidelity regarding the correspondence and comparability respectively.

For verification of the competence from the 3Co principle, the numerical result are compared with the experimental result by Fricke et al. [10], as well as the numerical result by Kubiczek [11]. The indicators here are the comparison of force-displacement curves, and the comparison of absorbed energy.

Fig. 21 shows the comparison of force-displacement curves from the experimental result and the numerical results. In Fig. 21, all numerical results agree well with experiment. The reasons for the difference between experimental result and numerical result is discussed by Kubiczek in [11], including the influence of friction, manufacturing, and so on. As a large complex structure, its numerical model can hardly represent every detail in the real experiment. Hence, the numerical result from Kubiczek has already shown very good performance. Comparing with the results from Kubiczek and the experiment, the results from both the shell-only model and the beam & shell model shows good performance as well, since they are quite close to each other.

Since the mesh size applied in this section (34.2 mm) is much larger than that used in Section 4 (5 mm), it is hard to include very local material behaviors with high accuracy. Normally, for relatively larger mesh size, it is hard for the numerical structure to keep high sensitivity to local material behaviors, such as necking or initiation of cracks [46,47]. Hence, for numerical investigation for large complex structure, the energy absorption is also used to check the results, see Fig. 22. From the comparison, the performances of the numerical models concerning energy absorption are close to each other. Among them the beam & shell model has better performance than the shell-only model during the collision of the outer hull. After that, their performances are similar until the displacement is close to 1200 mm. In this comparison, the difference

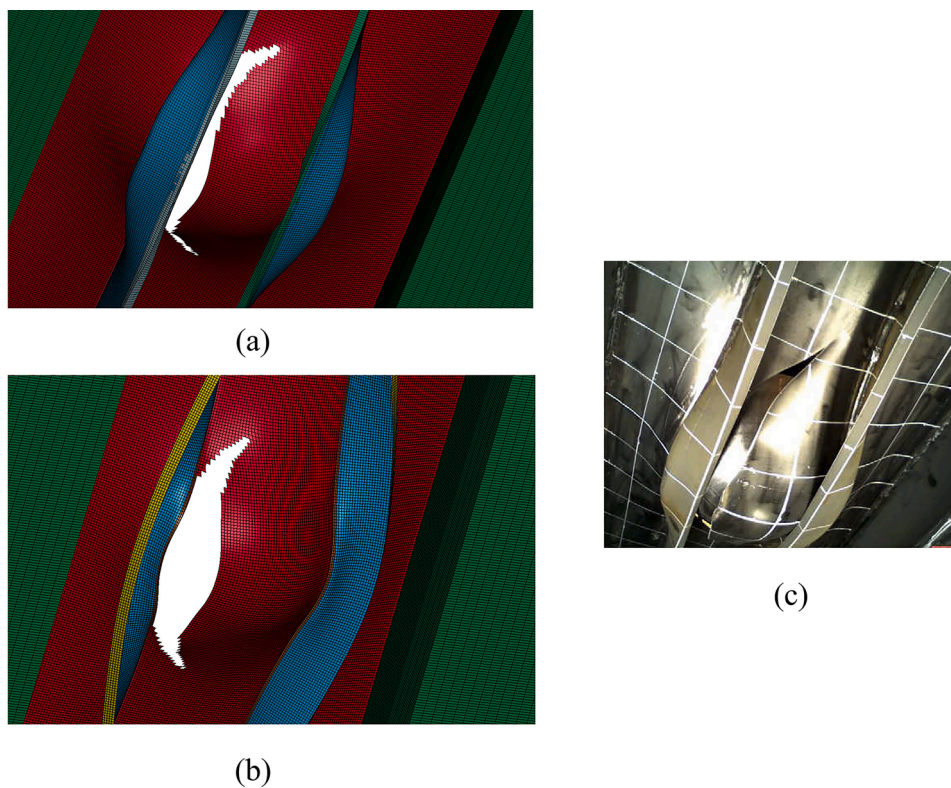


Fig. 17. The post-collision geometry from: (a) numerical simulation with beam & shell model, (b) numerical simulation with shell-only model, (c) the experiment [42].

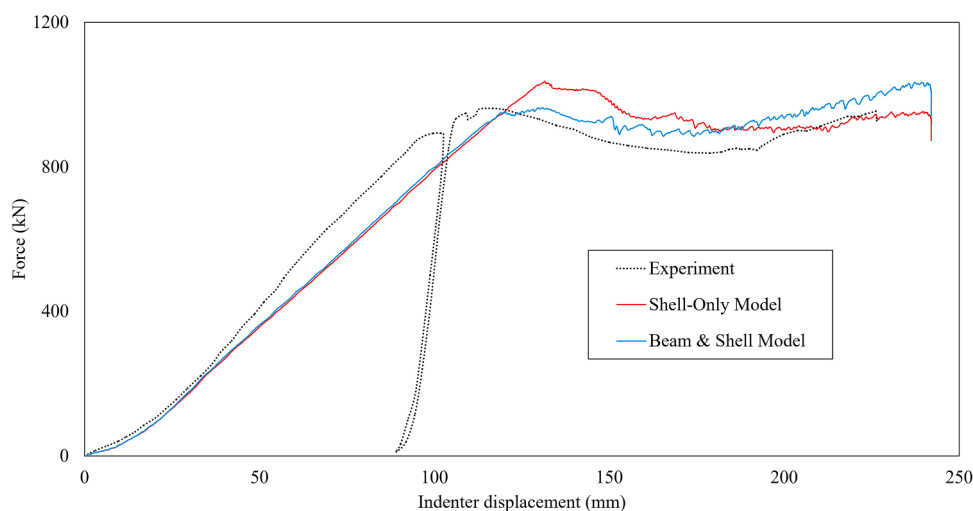


Fig. 18. Force-displacement from the experimental result and numerical models.

between experimental and numerical results also becomes larger when displacement is close to 1200 mm. This is due to the complexity of the collision between indenter and the inner hull, where the second stiffened panel receives collision. At this moment, uncertainties increase significantly compared with the collision of the outer hull (when only the first stiffened panel receive collision). Such condition is the same for the force-displacement result as well.

7. Discussion

Although bulb flats have been numerically modelled in many ship structural analysis, whether a bulb flat model should be accepted and

applied is seldom discussed. Thus, it is worthwhile to investigate the evaluation of numerical models, which can be accomplished by fidelity assessment. However, there has been no systematic assessment regarding the fidelity of bulb flat model. To enable the systematic fidelity assessment for bulb flat models, sufficient information, as well as an assessment strategy, are required. In this study, a framework called the “3Co principle” is presented. From the 3Co principle, the fidelity of a bulb flat is assessed with three characteristics: correspondence, comparability and competence. Each characteristic has its own indicators. By examining the indicators, the fidelity of the models can be assessed in a comparative way, which is suitable for fidelity determination [33]. The indicators and comparative results in this study are

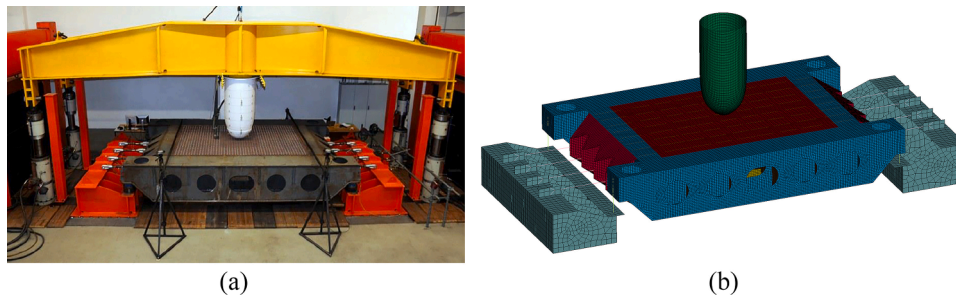


Fig. 19. (a): the test set-up of the large-scale experiment [10] and (b): the numerical model for the large-scale experiment.



Fig. 20. The bulb flats in the numerical model of large structure, modelled with shell-only model (left half) and beam & shell model (right half). Shell thickness and beam prism are shown here.

summarized in Table 7. The comparative results include three levels: “Same”, “Almost the same” and “which one is better”. “Same” means that the results are identical. “Almost the same” means that the results are very close to each other, which can be the difference of relative errors being less than 1% in quantitative results, or very few differences in qualitative results. “Which one is better” means that one of them has significantly better results than others, like more than 1% in quantitative results, or critically better performance in qualitative results.

In existing literature, the bulb flat models are not described with sufficient detail and thus cannot provide enough information for the fidelity assessment. A milestone study showing whether an indicator used in this study has also been mentioned in existing literatures is summarized in Table 8. Moreover, whether enough information is provided, as well as whether a systematic fidelity assessment is achieved in

these literatures, are also summarized in Table 8. Depending on different application conditions, the indicators are not supposed to be the same among all literatures. Therefore, the milestone study in Table 8 can provide an overview about the state of art regarding fidelity assessment for bulb flat models, yet more comprehensive investigation should be carried out based on individual conditions.

In this study, two bulb flat models, namely the shell-only model and the beam & shell model, together with their parameters, layouts and configurations, are described with details. In addition, the two models are applied in 3 scenarios and verified against analytical or experimental results. With sufficient information, these two models are used as examples for the fidelity assessment. From Section 3 to Section 6, the fidelities of the shell-only model and the beam & shell model are gradually assessed via the 3Co principle:

At the beginning, the fidelity in creating numerical models should be assessed. The creation of the bulb flat models is shown in Section 3. During the creation of models, the correspondence and comparability from the 3Co principle are considered. Thus, most physical parameters are the same as that from real components, while the layout of the real components is also properly described in the models. If subcomponents of the model are created with ‘equivalent’ form, the parameters and configurations are defined referring to the indicators.

During the creation of numerical models, their feasibilities should be considered, such as its computational cost. Considering computational cost, the shell-only model is created with reduced fidelity, while the beam & shell model does not have the same problem, see Fig. 9. The reduction of fidelity from the shell-only model leads to larger error in sectional parameters, which can be one of the reasons for different performance between the two models.

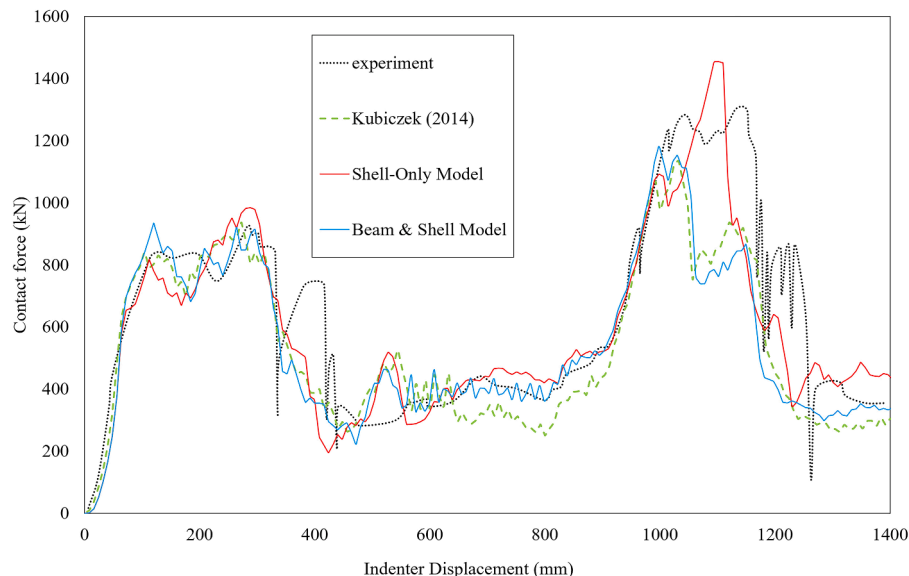


Fig. 21. Comparison of force-displacement curves from experiment and the numerical models. The numerical result from Kubiczek [11] is also included.

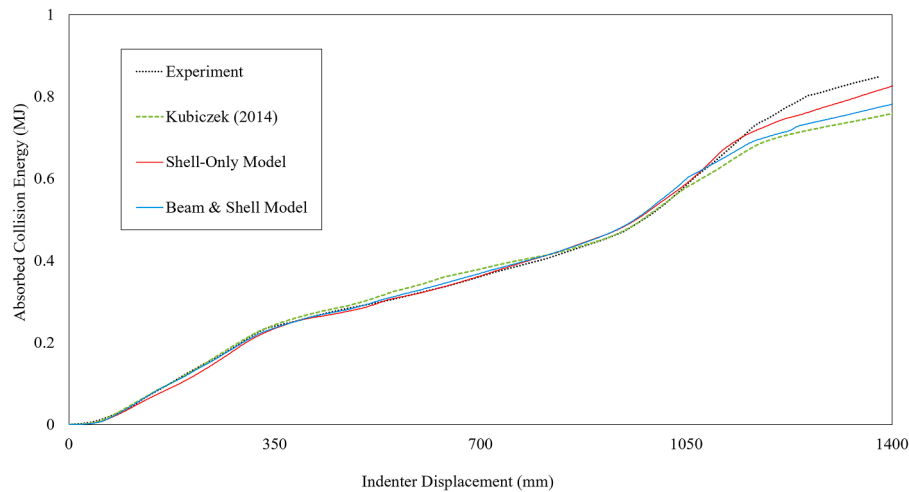


Fig. 22. Comparison of the absorbed collision energy from experiment and the numerical models. The numerical result from Kubiczek [11] is also included.

Table 7 Indicators and comparative results for fidelity in this study.

Characteristics	Indicators	Comparative results in this study
Correspondence	Cross-section area.	Same
	Area moment of inertia.	Almost the same
	Material properties.	Same
	Dimensions.	Same
Comparability	Outline shape.	Beam & shell model is better.
	Position of subcomponent.	Beam & shell model is better.
	Arrangement of subcomponents.	Beam & shell model is better.
	Boundary conditions.	Same
Competence	Deflection.	Almost the same
	Deformation.	Beam & shell model is better.
	Force-displacement results.	Almost the same
	Absorbed energy.	Almost the same

Table 8 A milestone study about fidelity assessment in existing literatures.

Literatures	Indicators for correspondence (in the literature / in this study)	Indicators for comparability (in the literature / in this study)	Indicators for competence (in the literature / in this study)	Enough information for rebuild or systematic fidelity assessment?
[3]	4 / 4	2 / 4	1 / 4	No
[4]	1 / 4	1 / 4	2 / 4	No
[6]	3 / 4	2 / 4	4 / 4	No
[7]	1 / 4	2 / 4	2 / 4	No
[11]	1 / 4	2 / 4	3 / 4	No
[12]	4 / 4	3 / 4	1 / 4	No
[13]	3 / 4	3 / 4	2 / 4	No
[14]	4 / 4	2 / 4	2 / 4	No

When the numerical models are created, their fidelities should be further assessed by verifications against analytical results or existing experimental results. In this study, two models are verified against analytical results in Section 4. The indicator is the deflection on specific points on the bulb flats, which is categorized in the competence from the 3Co principle. By examining the numerical results relevant to this indicator, the relative errors against analytical results are all lower than 3%. The performance of the beam & shell model is very close to that of the shell-only model.

For the verification against existing experimental results, the introduced bulb flat models are applied in two scenarios in this study.

Application of the models in a stiffened panel is verified with test results in Section 5, which closely related to non-linear ship structural analysis. The indicators here include post-collision deformation and force-displacement curve, which also belong to the competence from the 3Co principle. Via these indicators, the beam & shell model shows better performance than the shell-only model. Application of the models in a large complex structure is verified with test results in Section 6. Same as that in Section 5, this is closely related to non-linear ship structural analysis as well. The indicators here include force-displacement curves and absorbed energy, which belong to the competence from the 3Co principle as well. Via these indicators, both models show good performance, while the beam & shell model has slightly better performance than the shell-only model.

Summarizing the discussions above, with the 3Co principle and sufficient information, the fidelities of the two bulb flat models, during their creation and verification, are systematically assessed in this study. This is accomplished by comparing their numerical configurations or results with real components, analytical results, or test results, see Table 7. Other than that, additional methods can be applied to quantify the assessment results. This includes quantification methods to quantify all the indicators, and multi-criteria decision-making methods to coordinate the individual quantified results.

8. Conclusion

The aim of this study is to enable systematic fidelity assessment for bulb flat models in non-linear ship structural analysis, which can accomplish the evaluation of the numerical models and help the decisions for their acceptance and application. To achieve this, two things are essential: proper assessment strategy, and sufficient information. Hence, in this study, a “3Co principle” is introduced as a framework for the fidelity assessment, while two bulb flat models are described with their details and performances to provide sufficient information. The conclusions are as follows:

- In the 3Co principle, creation and verification are both considered for the bulb flat models. This means, not only the physical attributes of the models, but also their configuration in numerical software, as well as their performance, should be compared with that from real components to show their closeness. This closeness reveals the fidelity of the models.
- The 3Co principle includes three characteristics: correspondence, comparability and competence. These characteristics reveal the fidelity of the models via their quantitative parameters, qualitative descriptions, and performance in application. Each characteristic

contains multiple indicators to examine the model. Hence the 3Co principle can provide a framework for the systematic fidelity assessment.

- The two bulb flat models, namely the shell-only model and the beam & shell model, are both described with their parameters, configurations, and arrangements. Moreover, these two models are both verified against analytical results, as well as test results from two existing tests. With these descriptions and results, sufficient information is retrieved, which is essential for the fidelity assessment.
- Through the fidelity assessment, both bulb flat models show satisfying results. Compared with the shell-only model, the beam & shell model has better fidelity, which is more recommended for application.
- In study, the fidelities of the bulb flat models are assessed in a comparative way. Comparing the two bulb flat models, minor differences can lead to different performance in applications. Therefore, it is important to assess the fidelity of the models before application in complex scenarios, such as non-linear ship structural analysis.
- Due to the comparative way when assessing fidelities of the models, it is challenging to achieve quantitative results for fidelity assessment. However, 3Co principle provides an open framework for quantitative fidelity assessment. To achieve a quantitative fidelity assessment, more methods can be integrated into the framework in the future.

With the 3Co principle introduced in this study, as well as sufficient information during creation and verification, it is possible to systematically assess the fidelities of bulb flat models. The results of the presented research are believed to provide a sound basis for the use of bulb flat models in future applications regarding non-linear ship structural analysis. Such applications include simulation, optimization or machine learning with desired level of model fidelity.

Funding

The presented research is funded by the Deutsche Forschungsgemeinschaft (DFG, German Research Foundation)—project number 398019838. It is stated that all funders are not responsible for any of the content of this publication.

CRedit authorship contribution statement

Shi Song: Writing – original draft, Visualization, Validation, Software, Resources, Project administration, Methodology, Investigation, Formal analysis, Data curation, Conceptualization. **Sören Ehlers:** Writing – review & editing, Validation, Supervision, Resources, Project administration, Methodology, Investigation, Funding acquisition, Formal analysis, Conceptualization. **Moritz Braun:** Writing – review & editing, Validation, Supervision, Resources, Project administration, Methodology, Investigation, Formal analysis, Conceptualization. **Franz von Bock und Polach:** Writing – review & editing, Validation, Supervision, Resources, Project administration, Investigation, Formal analysis. **Aditya Rio Prabowo:** Writing – review & editing, Validation, Investigation.

Declaration of competing interest

The authors declare that they have no known competing financial interests or personal relationships that could have appeared to influence the work reported in this paper.

Data availability

Data will be made available on request.

References

- [1] Fischer C, Fricke W. Fatigue assessment of joints at bulb profiles by local approaches 2015:251–9.
- [2] W Fricke, Lilienfeld-toal A Von, H Paetzold, Fatigue strength investigations of welded details of stiffened plate structures in steel ships. *Int. J. Fatigue* 34 (2012) 17–26, <https://doi.org/10.1016/j.ijfatigue.2011.01.021>.
- [3] E Avi, I Lillemäe, J Romanoff, A Niemi, Equivalent shell element for ship structural design, *Ships Offshore Struct.* 10 (2015) 239–255, <https://doi.org/10.1080/17445302.2013.819689>.
- [4] M Korgesaar, K Tabri, H Naar, E Reinhold, Ship collision simulations using different fracture criteria and mesh size. *Vol. 4A Struct. Saf. Reliab. Am. Soc. Mech. Eng.* (2014) 1–9, <https://doi.org/10.1115/OMAE2014-23576>.
- [5] Bars A, Fricke W, Paetzold H, Rörup J. Fatigue strength of stiffener end connections : a comparative study of bulb fatigue strength of stiffener end connections : a comparative study of bulb flats and angle bars 2010.
- [6] Z Yu, I Amdahl, S. Løset, Evaluation of load-carrying capacity of a submersible platform subjected to accidental ice impacts, in: *Dev collis grounding ships offshore struct - Proc 8th Int Conf Collis grounding ships offshore struct ICCGS 2019, 2020*, pp. 212–218, <https://doi.org/10.1201/9781003002420-27>.
- [7] HS Alsos, J Amdahl, OS. Hopperstad, On the resistance to penetration of stiffened plates, Part II: Numerical analysis, *Int. J. Impact. Eng.* 36 (2009) 875–887, <https://doi.org/10.1016/j.ijimpeng.2008.11.004>.
- [8] S. Ehlers, A procedure to optimize ship side structures for crashworthiness, *Proc. Inst. Mech. Eng. Part M J. Eng. Marit. Environ.* 224 (2010) 1–11, <https://doi.org/10.1243/14750902JEME179>.
- [9] S. Ehlers, A particle swarm algorithm-based optimization for high-strength steel structures, *J. Sh. Prod. Des.* 28 (2012) 209–219, <https://doi.org/10.5957/JSPD.28.1.110029>.
- [10] Fricke W, Schöttelndreyer M, Tautz I. Validierung von Kollisionsberechnungen durch Großversuche an Konstruktionsvarianten von Seitenhüllen - Abschlussbericht BMWI- Vorhaben ELKOS 03SX284B. 2014. <https://doi.org/10.2314/GBV:819246204>.
- [11] JM. Kubiczek, *Anwendung Des GISSMO-Versagensmodells Auf Schiffbauliche Strukturen*, Technische Universität Hamburg-Harburg, 2014.
- [12] Wilmer III A. Analytic expression of the buckling loads for stiffened plates with bulb-flat flanges. Naval Postgraduate School, 2003. <https://apps.dtic.mil/sti/pdfs/ADA417591.pdf>.
- [13] M Bobeldijk, S Dragt, M Hoogeland, J. van Bergen, Assessment of the technical safe limit speed of a non-ice-strengthened naval vessel with representative and alternative side shell designs in ice-infested waters, *Ships Offshore Struct.* 16 (2021) 275–289, <https://doi.org/10.1080/17445302.2021.1912475>.
- [14] J Cui, D Wang, N. Ma, Elastic buckling of stiffened panels in ships under bi-axial compression, *Ships Offshore Struct* 12 (2017) 599–609, <https://doi.org/10.1080/17445302.2016.1189140>.
- [15] JW Ringsberg, J Amdahl, BQ Chen, S-R Cho, S Ehlers, Z Hu, et al., MARSTRUCT benchmark study on nonlinear FE simulation of an experiment of an indenter impact with a ship side-shell structure, *Mar Struct* 59 (2018) 142–157, <https://doi.org/10.1016/j.marstruc.2018.01.010>.
- [16] JW Ringsberg, I Darie, K Nahshon, G Shilling, M Augusto, S Benson, et al., The ISSC 2022 committee III . 1-Ultimate strength benchmark study on the ultimate limit state analysis of a stiffened plate structure subjected to uniaxial compressive loads, *Mar Struct.* 79 (2022) 103026, <https://doi.org/10.1016/j.marstruc.2021.103026>.
- [17] JA Durlak, EP. DuPre, Implementation matters: A review of research on the influence of implementation on program outcomes and the factors affecting implementation, *Am. J. Comm. Psychol.* 41 (2008) 327–350, <https://doi.org/10.1007/s10464-008-9165-0>.
- [18] FJ Moncher, RJ. Prinz, Treatment fidelity in outcome studies, *Clin. Psychol. Rev.* 11 (1991) 247–266, [https://doi.org/10.1016/0272-7358\(91\)90103-2](https://doi.org/10.1016/0272-7358(91)90103-2).
- [19] D Jones, C Snider, A Nassehi, J Yon, B. Hicks, Characterising the Digital Twin: A systematic literature review, *CIRP. J. Manuf. Sci. Technol.* 29 (2020) 36–52, <https://doi.org/10.1016/j.cirpj.2020.02.002>.
- [20] LFCS Durão, S Haag, R Anderl, K Schützer, E. Zancul, Digital twin requirements in the context of industry 4.0, *IFIP. Adv. Inf. Commun. Technol.* 540 (2018) 204–214, https://doi.org/10.1007/978-3-030-01614-2_19.
- [21] E VanDerHorn, S. Mahadevan, Digital Twin: Generalization, characterization and implementation, *Decis. Support. Syst.* 145 (2021) 113524, <https://doi.org/10.1016/j.dss.2021.113524>.
- [22] B Schleich, N Anwer, L Mathieu, S. Wartzack, Shaping the digital twin for design and production engineering, *CIRP Ann - Manuf. Technol.* 66 (2017) 141–144, <https://doi.org/10.1016/j.cirp.2017.04.040>.
- [23] R. Vinuesa, High-fidelity simulations in complex geometries: Towards better flow understanding and development of turbulence models, *Results. Eng.* 11 (2021) 100254, <https://doi.org/10.1016/j.rineng.2021.100254>.
- [24] V Vilceanu, S Chawdhury, G. Morgenthal, A novel partitioned numerical coupling between vortex particle method–structure–smoothed particle hydrodynamics models for wind-induced vibration analysis, *Results. Eng.* 23 (2024) 102435, <https://doi.org/10.1016/j.rineng.2024.102435>.
- [25] AS Milaković, F Li, von Bock und Polach RUF, S. Ehlers, Equivalent ice thickness in ship ice transit simulations: overview of existing definitions and proposition of an improved one, *Sh. Technol. Res.* 67 (2020) 84–100, <https://doi.org/10.1080/09377255.2019.1655260>.
- [26] EL Ntantis, V. Xezonakis, Improving transonic performance with adjoint-based NACA 0012 airfoil design optimization, *Results. Eng.* 24 (2024) 103189, <https://doi.org/10.1016/j.rineng.2024.103189>.

- [27] N Kroll, M Abu-Zurayk, D Dimitrov, T Franz, T Führer, T Gerhold, et al., DLR project Digital-X: towards virtual aircraft design and flight testing based on high-fidelity methods, *CEAS. Aeronaut. J.* 7 (2016) 3–27, <https://doi.org/10.1007/s13272-015-0179-7>.
- [28] A Ojo, M Collu, A. Coraddu, Multidisciplinary design analysis and optimization of floating offshore wind turbine substructures: A review, *Ocean Eng* 266 (2022) 112727, <https://doi.org/10.1016/j.oceaneng.2022.112727>.
- [29] S Hiremath, Y Zhang, L Zhang, TW. Kim, Machine learning approach to evaluating impact behavior in fabric-laminated composite materials, *Results. Eng.* 23 (2024) 102576, <https://doi.org/10.1016/j.rineng.2024.102576>.
- [30] X Luo, A Kareem, L Yu, S Yoo, A machine learning-based characterization framework for parametric representation of liquid sloshing, *Results. Eng.* 18 (2023) 101148, <https://doi.org/10.1016/j.rineng.2023.101148>.
- [31] Jiang C xia, Liu Y bo, Wang Z yuan, S Chen, Cai S ze, Q Gao, et al., A multi-fidelity prediction model for vertical bending moment and total longitudinal stress of a ship based on composite neural network, *J. Hydrodyn* 35 (2023) 27–35, <https://doi.org/10.1007/s42241-023-0008-0>.
- [32] L Huang, B Pena, Y Liu, E. Anderlini, Machine learning in sustainable ship design and operation: A review, *Ocean Eng.* 266 (2022) 112907, <https://doi.org/10.1016/j.oceaneng.2022.112907>.
- [33] M. Giselle Fernández-Godino, Review of multi-fidelity models, *Adv. Comput. Sci. Eng.* 1 (2023) 351–400, <https://doi.org/10.3934/acse.2023015>.
- [34] C. Mowbray, Fidelity criteria: development, measurement, and validation, *Am. J. Eval.* 24 (2003) 315–340, [https://doi.org/10.1016/S1098-2140\(03\)00057-2](https://doi.org/10.1016/S1098-2140(03)00057-2).
- [35] International Organization for Standardization. ISO 657-19:1980. Hot-rolled steel sections; Part 19 : Bulb flats (metric series); Dimensions, sectional properties and tolerances. vol. 1980. 1980.
- [36] S Ehlers, H Remes, A Klanac, H. Naar, A multi-objective optimisation-based structural design procedure for the concept stage - A chemical product tanker case study, *Sh Technol Res* 57 (2010) 182–197, <https://doi.org/10.1179/str.2010.57.3.004>.
- [37] S Shadkam, E Ranjbarbarnodeh, M. Iranmanesh, Effect of sequence and stiffener shape on welding distortion of stiffened panel, *J. Constr. Steel. Res.* 149 (2018) 41–52, <https://doi.org/10.1016/j.jcsr.2018.07.010>.
- [38] M Ventura, C. Guedes Soares, Modelling stiffeners of ship hull structures, *Proc. Inst. Mech. Eng. Part M J. Eng. Marit. Environ.* 227 (2013) 155–166, <https://doi.org/10.1177/1475090212462524>.
- [39] M Gellert, WH. Wittrick, A finite prism element for stability analysis of bulb flat stiffeners, *Int. J. Mech. Sci.* 17 (1975) 469–473, [https://doi.org/10.1016/0020-7403\(75\)90046-6](https://doi.org/10.1016/0020-7403(75)90046-6).
- [40] DNV. Rules for Classification Ships - Part 3 Hull, Chapter 3 Structural design principles 2017:81–2.
- [41] IACS. UR S35 buckling strength assessment of ship structural elements - New Feb 2023. vol. 35. 2023.
- [42] HS Alsos, J. Amdahl, On the resistance to penetration of stiffened plates, Part I – Experiments, *Int. J. Impact. Eng.* 36 (2009) 799–807, <https://doi.org/10.1016/j.ijimpeng.2008.10.005>.
- [43] M Debeurre, A Grolet, O. Thomas, Extreme nonlinear dynamics of cantilever beams: effect of gravity and slenderness on the nonlinear modes, *Nonlinear. Dyn.* 111 (2023) 12787–12815, <https://doi.org/10.1007/s11071-023-08637-x>.
- [44] OA Bauchau, J.L. Craig, *Structural analysis: with applications to aerospace structures*, Springer Dordrecht Heidelberg London New York, 2009.
- [45] C Kober, V Adomat, M Ahanpanjeh, M Fette, JP. Wulfsberg, Digital twin fidelity requirements model for manufacturing, *RepoUni-HannoverDe* (2022).
- [46] S Ehlers, P. Varsta, Strain and stress relation for non-linear finite element simulations, *Thin-Walled Struct.* 47 (2009) 1203–1217, <https://doi.org/10.1016/j.tws.2009.04.005>.
- [47] B Wiegard, S. Ehlers, Pragmatic regularization of element-dependent effects in finite element simulations of ductile tensile failure initiation using fine meshes, *Mar. Struct.* 74 (2020) 102823, <https://doi.org/10.1016/j.marstruc.2020.102823>.